Melt Spinning of Metallocene Catalyzed Polypropylenes. II. As-Spun Filament Structure and Properties

ERIC BRYAN BOND, JOSEPH E. SPRUIELL

Center for Materials Processing and Department of Materials Science and Engineering, The University of Tennessee, 434 Dougherty Engineering Building, Knoxville, Tennessee 37996-2200

Received 23 December 2000; accepted 1 February 2001

ABSTRACT: The melt spinning of metallocene catalyzed isotactic polypropylene (miPP) resins was investigated. The as-spun filament properties from six miPP resins were studied with melt flow rates (MFR) between 10 and 100, and a Ziegler–Natta catalyzed isotactic polypropylene (zniPP) resin with a MFR of 35 was studied for a comparison. Generally, as the molecular weight increased the filament density increased, the birefringence decreased, the tensile strength decreased, and the elongation to break increased. As the spinning speed increased, the density, birefringence, tensile strength, and crystalline and noncrystalline orientation functions generally increased. However, the low MFR miPP and the zniPP resin had decreases in the birefringence and tensile strength with an increase of the spinning speed. The miPP resins were found to have breaking tensile strengths up to 50% higher than the zniPP resin at similar spinning speeds. The observed fiber properties were explained based on the nature and orientation of noncrystalline portions of the fibers. © 2001 John Wiley & Sons, Inc. J Appl Polym Sci 82: 3237–3247, 2001

Key words: metallocene; polypropylene; melt spinning; fiber

INTRODUCTION

Earlier studies[1–6] reported on the effect of numerous process and materials variables on the structure and properties of melt-spun filaments prepared from Ziegler–Natta catalyzed isotactic polypropylene (zniPP).

The present series of two articles describes the structure and properties of as-spun filaments produced from a series of metallocene catalyzed iPP (miPP) resins. In the first article of this series[7] we presented and interpreted on-line data for the same set of iPP resins studied in the present report. Furthermore, the effect on the development of the fiber structure of the molecular architecture, which includes the molecular weight characteristics, defect content, and defect type, was discussed for these resins in the first part of this series.[7] In the present article we further examine the structure developed in the as-spun filaments and the implications of the structure development on the tensile mechanical properties of the as-spun filaments.

EXPERIMENTAL

Resin Characteristics

The resin characteristics for the present set of iPP resins, which included the molecular weight, molecular weight distribution (MWD), and stereoregularity, were described earlier.[7] The basic thermal behavior of the resins, including the

Correspondence to: J. E. Spruiell.
Contract grant sponsor: ExxonMobil Chemical Company.

Journal of Applied Polymer Science, Vol. 82, 3237–3247 (2001)

melting and crystallization temperatures and heat of fusion, is important information that was also presented in part I.[7]

Melt Spinning

Filaments were spun using the same equipment as in our earlier studies, which can be found in those articles.[3–6] The specific procedures used for the preparation of the present filaments were described previously.[7] Briefly, the samples were all spun as monofilaments; the extrusion temperature and mass throughput were kept as constant and consistent as possible for all samples produced. The extrusion temperature was 210°C, and the mass throughput was 1.55 ± 0.03 g/min. The mass throughput was measured before and after each set of fibers was spun. The spinning speeds were computed from the continuity equation. The diameter used in calculating the spinning speed came from the on-line steady-state diameter measured 2.20 m from the spinneret. The final, off-line relaxed diameters were up to 25% larger than the on-line diameters, depending on the spinning conditions. The off-line diameters were used for calculating the cross-sectional area of the fibers for the measurement of the mechanical properties.

Filament Characterization

Initial studies indicated that the fiber properties were not constant with time after the initial spinning process, but the fiber properties became relatively constant after conditioning for a period of time at room temperature. Consequently, all reported as-spun filament characterizations in the present article were carried out after a 30-day room temperature conditioning period.

The as-spun filaments were characterized by measurements of the density, birefringence, wide angle and small angle X-ray patterns, and tensile mechanical properties. The experimental procedures were described in our previous articles.[3–7] Briefly, the density was measured in an isopropyl alcohol/water density gradient column maintained at 23°C. The birefringence values were measured using a polarizing microscope equipped with a Berek compensator and a filar eyepiece. The tensile tests were run using fibers with an initial gauge length of 25 mm and a crosshead speed of 50 mm/min. The reported results are the average values determined from no less than 10 tensile test specimens for each condition.

Determination of Orientation Functions

The average molecular orientation of the crystallites was given a quantitative description using the Hermans orientation function.[8,9] The orientation function (f_c) describes the orientation of the polymer chains relative to the fiber axis; it is defined as

$$f_c \equiv \frac{3\ \overline{\cos^2\phi} - 1}{2} \qquad (1)$$

where $\cos^2\phi$ is the average cosine squared value of the angle ϕ between the chain axis and the fiber axis. When $f_c = 1$, the chains are parallel to the fiber axis, while $f_c = 0$ represents a random orientation of the chains. For the crystalline fraction, the value of $\cos^2\phi$ was evaluated from azimuthal X-ray intensity measurements on the (110) and (040) reflections as described for iPP by Wilchinsky[10] and Alexander.[11]

Stein and Norris[12] showed that the orientation of crystalline and amorphous domains of a semicrystalline polymer can be related to the birefringence by

$$\Delta n = (1 - X_c) f_{\mathrm{nc}} \Delta^0_{\mathrm{nc}} + X_c f_c \Delta^0_c + \Delta n_{\mathrm{form}} \qquad (2)$$

where X_c is the crystalline fraction, f_{nc} is the noncrystalline orientation function, f_c is the crystalline orientation function, Δ^0_{nc} is the noncrystalline intrinsic birefringence, Δ^0_c is the crystalline intrinsic birefringence, and Δn_{form} is the form birefringence resulting from light interaction with the two phases. In semicrystalline polymers the form birefringence is small and is typically neglected.[12,13] For iPP, $\Delta^0_c = 0.0291$ and $\Delta^0_{nc} = 0.0600$.[14–16]

RESULTS AND DISCUSSION

Structure of As-Spun Filaments

The density of as-spun filaments as a function of the spinning speed is presented in Figure 1. For all resins the density increased with increasing spinning speed. The results in Figure 1 show that, although there were minor variations in the order of the resins at different spinning speeds, the overall behavior of the metallocene resins was to exhibit greater density at a given take-up velocity with increasing molecular weight and decreasing melt flow rate (MFR). The range of densities of

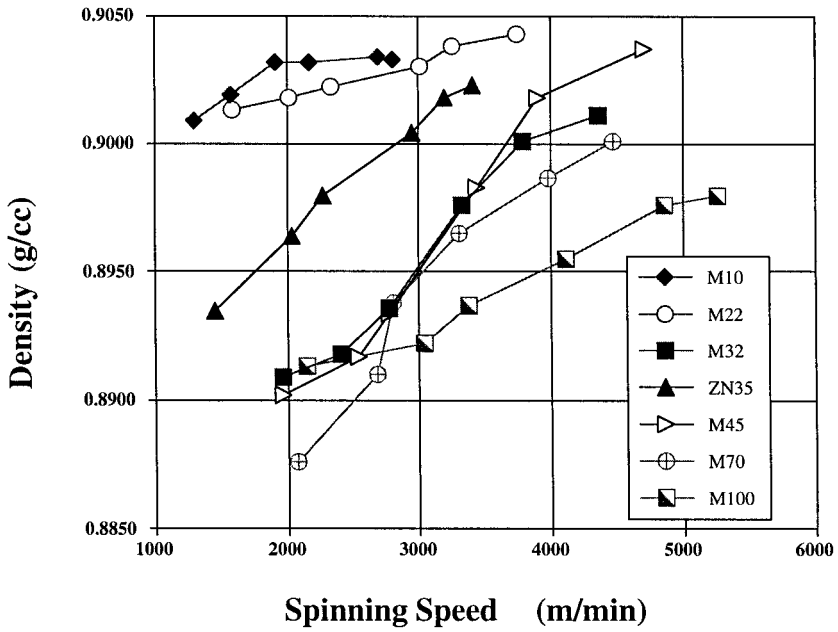

Figure 1 The density of the filaments versus the spinning speed.

these fibers was 0.8900–0.9050 g/cm^3, similar to previous studies of zniPP fibers.[3–6] The lower molecular weight resins showed a greater increase in density with the increase of the spinning speed within the range of take-up velocities studied, while the higher molecular weight resins started at a higher density and exhibited a smaller increase of density as the take-up velocity was increased. If the increase of density is interpreted as largely a result of an increase of crystallinity developed in the filaments, the higher densities suggest increased molecular orientation enhanced crystallization in the spin line with increased molecular weight and spinning speed. Higher molecular weight resins exhibited greater effects at lower take-up velocities, and the lower molecular weight materials required higher spinning speeds in order to develop equivalent crystallinity values.

Close inspection showed that the MWD was important in determining the filament densities. Specifically, the Ziegler–Natta resin with a MFR of 35 (ZN35) and the metallocene resin with a MFR of 45 (M45) had broader MWDs than the M32 resin. Although their MFRs were higher, the densities of M45 filaments were approximately equal to those of M32, while the densities of ZN35 filaments were higher. The polydispersities were 2.28 for M32, 2.83 for M45, and 3.29 for ZN35. Their weight-average molecular weights were 172,500 g/mol for M32, 164,500 g/mol for M45, and 189,100 g/mol for ZN35. The substantially higher density values of the M22 resin compared to ZN35 seemed a bit anomalous when considering the respective MWDs. The weight-average molecular weight of M22 was 192,100 g/mol and its polydispersity was 2.25. The parameter that we believe should be compared in order to explain the sequence of the density data is the elongational viscosity. Unfortunately, the elongational viscosity data for these resins was not available. However, M22 did exhibit a lower MFR and substantially higher complex viscosity over a wide range of frequencies than either M32 or ZN35, including at low frequencies as shown in Figure 2. This suggests that the elongational viscosity of M22 would also be higher than that of M32 or ZN35.

The birefringence results in Figure 3 show that as the spinning speed increased, the final birefringence increased for all resins except M10 and ZN35. The birefringence for M10 decreased, but that of ZN35 exhibited a modest maximum with increasing spinning speed in the range of spinning speeds investigated in this study. Figure 3 also indicates that the ultimate birefringence achieved at higher spinning speeds was generally increased with decreasing weight-average molecular weight.

Previous studies[1–6] stated that increasing molecular weight at similar MWD values produces higher birefringence values. This is presumably a

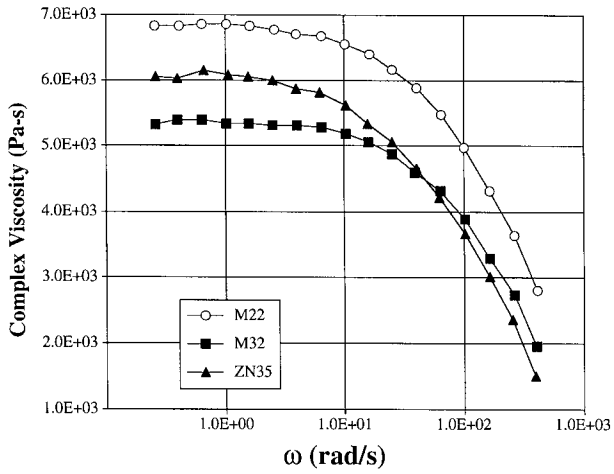

Figure 2 The complex viscosity versus the frequency for M22, M32, and ZN35.

result of more stress in the spin line when compared at the same spinning speed. We observed that the order of birefringence of the resins was a strong function of the spinning speed, as well as their molecular weight. In the lower spinning speed range the higher molecular weight resins tended to lead to higher birefringence values, as previously reported. However, at higher spinning speeds this trend was reversed, according to Figure 3. The on-line data shown previously indicated that the higher molecular weight resins crystallized closer to the spinneret and at higher temperatures at equivalent spinning speeds.[7] The molecules of the lower molecular weight (higher MFR) resins eventually became sufficiently oriented to allow the onset of crystallization, which was due to the melt being continuously elongated and cooled until crystallization began. In addition, crystallizing at a lower temperature meant crystallization was more rapid, which would tend to produce more tie molecules that are frozen in more effectively at the lower crystallization temperature. The behavior of the birefringence of the miPP resins can be understood on the basis of these considerations.

Earlier studies[3,5] on zniPP resins with different MWD values indicated that broad MWD samples developed a higher crystallinity (i.e., density) and lower final birefringence than did samples spun with narrow MWD resins with similar MFR. In these studies the filament birefringence values tended to decrease as the molecular weight decreased or the MWD broadened. Typical birefringence values were between 0.013 and 0.022; in the present studies the birefringence values ranged from 0.016 to 0.030. Clearly there were substantial differences in the birefringence values in the two sets of resins. However, it must be noted that the present set of miPP resins had very low polydispersities and a very narrow range of polydispersity values. Further, the resins used in the previous studies were all prepared with Ziegler–Natta catalysts. Therefore, it is not sur-

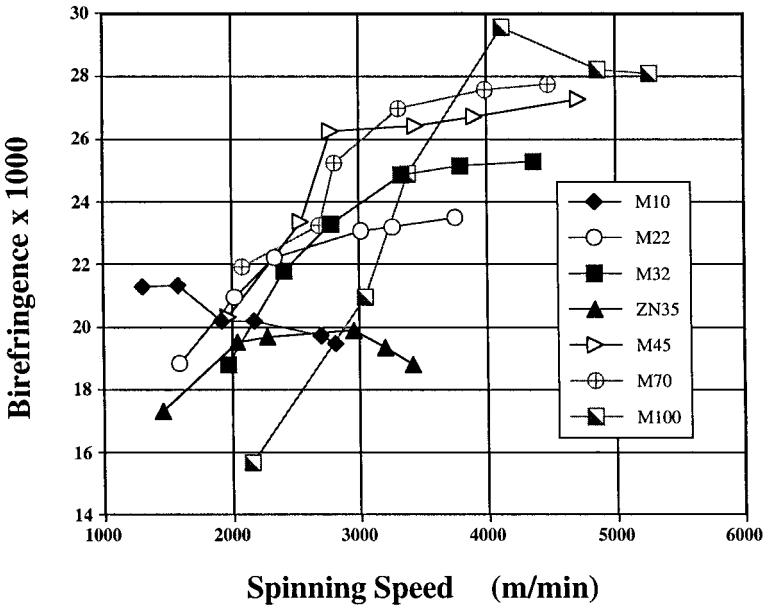

Figure 3 The birefringence of as-spun filaments versus the spinning speed.

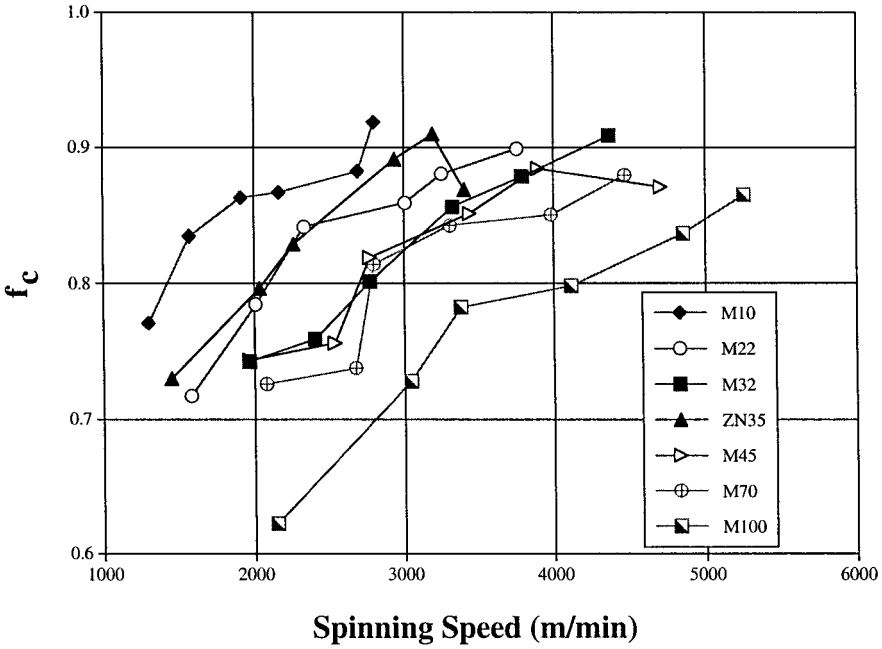

Figure 4 The crystalline orientation function versus the spinning speed.

prising that somewhat different behavior was observed.

In order to determine the origin of the higher birefringence in the miPP resins, the crystalline and noncrystalline orientation functions were determined for each fiber. The crystalline orientation function for the as-spun filaments is shown in Figure 4. The data show that, as the spinning speed increased, the crystalline orientation function generally increased in the range of spinning speeds studied for each resin. Moreover, as the molecular weight increased or the MFR decreased, the crystalline orientation function also tended to increase (i.e., the crystalline orientation function for M10 > M22 >, etc.) at the same spinning speed. The on-line birefringence studies in part I[7] showed that the higher molecular weight resins crystallized closer to the spinneret, which seemed to produce more highly oriented row nuclei and ultimately higher crystalline orientation according to the data in Figure 4.

The noncrystalline orientation function for each resin is shown in Figure 5. The value of the noncrystalline orientation function for the miPP resins increased with the spinning speed, except for the M10, which decreased as the spinning speed increased. Resin ZN35 also showed a decrease in the noncrystalline orientation function as a function of increasing spinning speed. Some of the miPP resins exhibited a slight maximum in the noncrystalline orientation function as the spinning speed was further increased. The M22 resin increased slightly, but not as dramatically, as the lower molecular weight resins. We previously showed that the crystallization temperature increased as the spinning speed increased for a given resin.[7] As the crystallization temperature increased, it apparently became possible for oriented noncrystalline chains to relax, which was due to increased thermal energy. At the lower crystallization temperatures the noncrystalline orientation was retained and contributed to the formation of higher birefringence in these filaments. The data suggested that there was a critical crystallization temperature above which the noncrystalline regions will relax for a given resin. The temperature at which the noncrystalline regions relax would likely depend on the molecular weight in some rough correspondence with the Williams–Landel–Ferry equation.

Figure 6 shows flat plate X-ray diffraction patterns of a few representative fiber samples. Note that the patterns indicate that the crystalline perfection increased with the increase of either the spinning speed or molecular weight. A well-developed α phase was present in the filaments that were melt spun from the higher molecular weight samples at all spinning speeds studied. As the spinning speed and molecular weight decreased the patterns showed considerable line broaden-

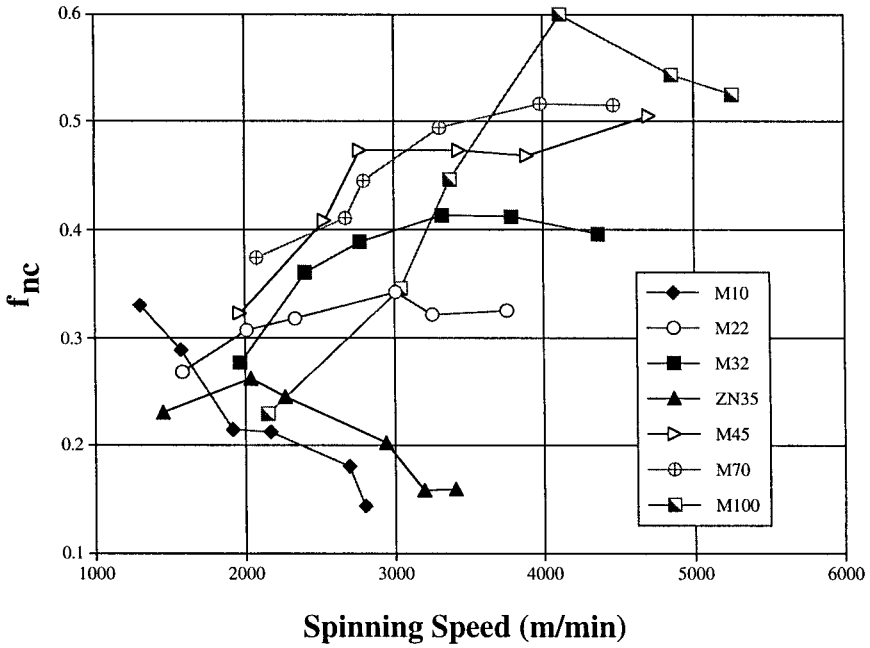

Figure 5 The noncrystalline orientation function versus the spinning speed.

ing, indicative of smaller crystal size. Finally, for the lower molecular weight resins and at the lower spinning speeds, the patterns indicated the presence of the oriented smectic form. Comparing the crystallization temperatures found in part I[7] with the present results showed that the observed differences in structure were consistent with changes in the crystallization temperature. Higher crystallization temperatures produced a better developed α phase. Because the lower molecular weight resins crystallized at lower temperatures at a given spinning speed, they re-

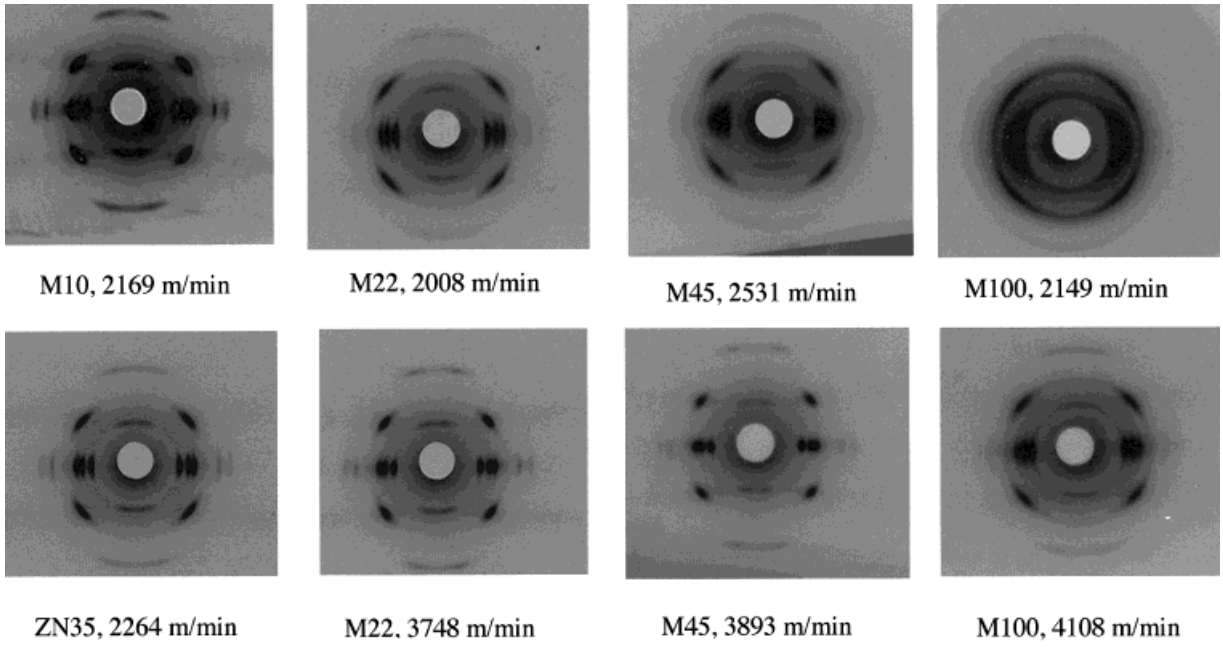

Figure 6 Flat plate wide angle X-ray spectroscopy patterns illustrating the effects of the take-up velocity, resin type, and resin molecular weight.

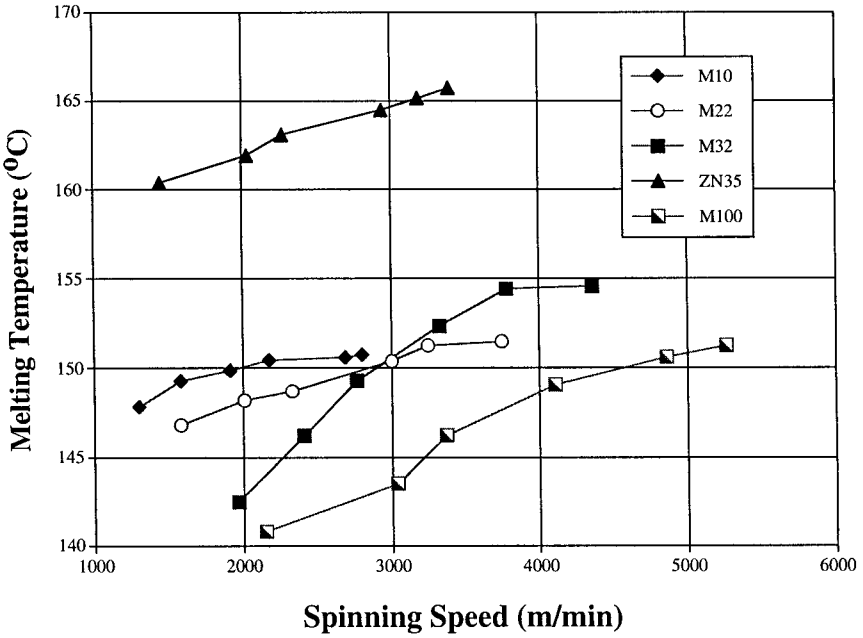

Figure 7 The fiber melting temperature versus the spinning speed.

quired higher spinning speeds to obtain a well-developed α phase than the higher molecular weight resins. As noted in part I,[7] the occurrence of the smectic phase was consistent with the fact often mentioned in the literature[17,18] that it appeared when the crystallization temperature was below about 70°C. Our data indicated that the occurrence of the smectic form in melt-spun fibers was little affected by the molecular characteristics, except as these characteristics influenced the crystallization temperature. In this regard, the miPP resins appeared to behave like very narrow distribution zniPP resins. The narrower distribution caused the crystallization temperature of the miPP resins to be lower than for broader distribution zniPP resins with similar weight-average molecular weight and/or MFR.

Finally, the melting temperature of each fiber as a function of the spinning speed is shown in Figure 7. As noted in in previous studies,[7,19] the melting temperature of the ZN35 resin was substantially above the values for the miPP resins. Figure 7 shows that this remained true for the filaments. Further, as the spinning speed was increased, the melting temperature increased for all resins. The melting temperature was known to be a function of the crystallization temperature through its dependence on the crystal lamella thickness. Because the crystallization temperature of each resin increased as the spinning speed was increased,[7] the melting temperature was expected to increase with the spinning speed. We note further that M32 and M100 showed a higher sensitivity of the melting temperature to the spinning speed than did M10 and M22. This fact suggested that molecular orientation had an effect on the melting temperature of the filaments (compare Fig. 3) that went beyond the effect of the crystallization temperature.

Tensile Mechanical Properties of Melt-Spun Filaments

The tensile modulus for each resin as a function of the spinning speed is shown in Figure 8. For all resins, the tensile modulus increased as the spinning speed increased. The results in Figure 8 indicate that the tensile modulus values for the resins in this study seemed to cluster near a common line as a function of the spinning speed. The tensile modulus is a function of both the crystallinity and overall molecular orientation. As the spinning speed increased, the crystallinity (i.e., density) and birefringence both increased for most of the resins. The tensile modulus increased in a manner consistent with the combination of these factors, even though the crystallinities and birefringence values were not independently identical for the resins at any given spinning speed.

The tensile strengths of the fibers in this study are shown in Figure 9 as a function of the spin-

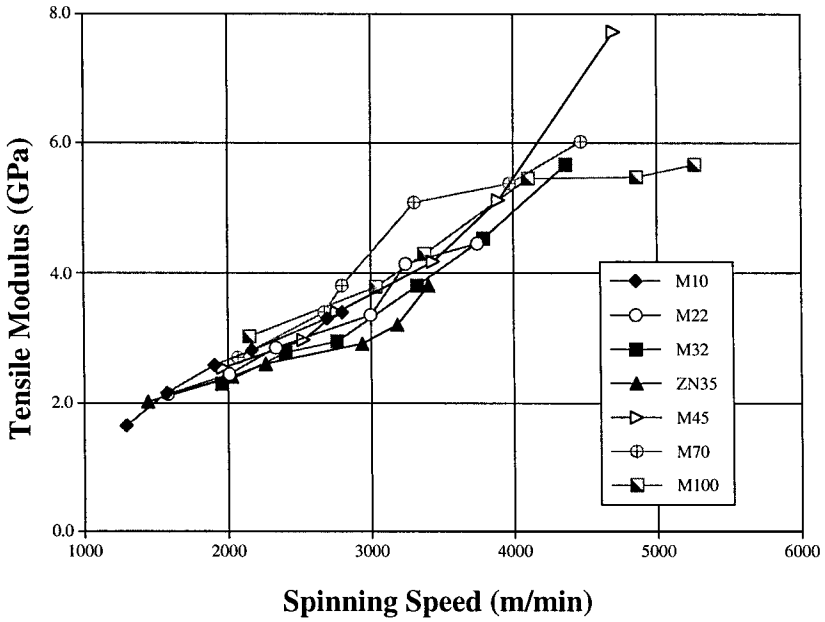

Figure 8 The tensile modulus versus the spinning speed.

ning speed. Except for M100 at the lowest spinning speed, all filaments prepared from miPP resins had significantly higher tensile strength than those prepared from ZN35. In general, the tensile strength increased as the spinning speed increased with the exception of M10 and ZN35. The tensile strength of M10 decreased slightly as the spinning speed increased, while the tensile strength of ZN35 exhibited a modest maximum versus the spinning speed as did some of the lower molecular weight resins.

Tensile strength depends on the number of tie molecules connecting the various crystallites and the chain extension of these molecules. Because the crystallites act as an anchor for the tie molecules, which allows the stress to be transferred

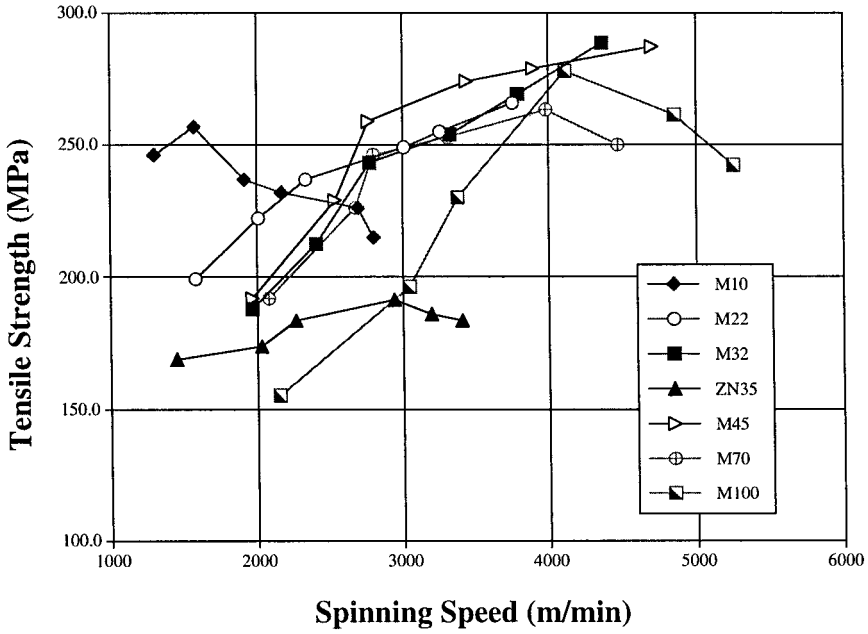

Figure 9 The tensile strength versus the spinning speed.

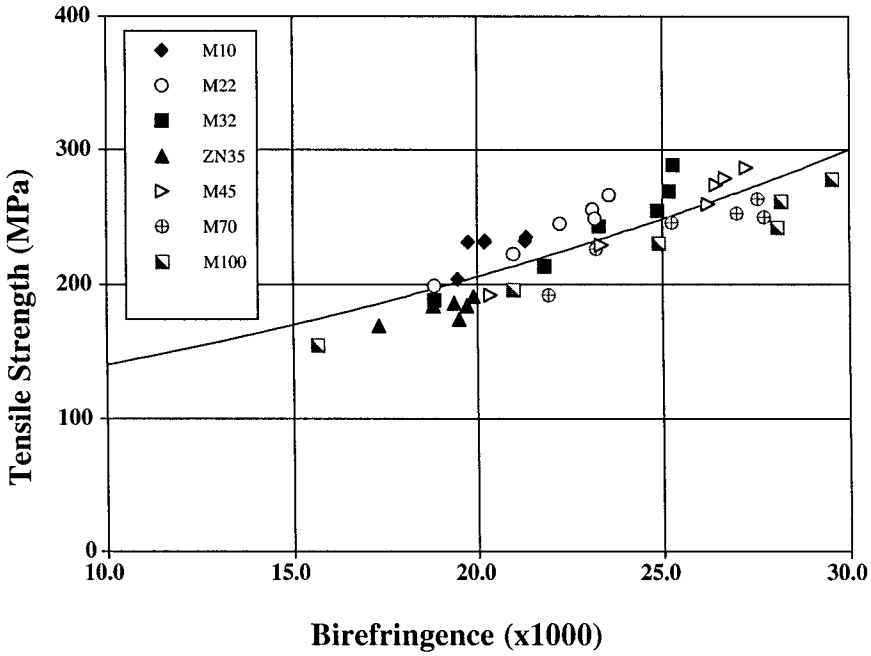

Figure 10 The fiber tensile strength versus the total fiber birefringence.

throughout the material during deformation, tensile strength is also dependent upon the crystallinity to some extent. A further contributing factor may be that M10 and ZN35 crystallized at significantly higher temperatures than the other resins in the spin line, as pointed out in part I.[7] Earlier, the decrease in the noncrystalline orientation function was attributed to the higher crystallization temperatures. Taking this correlation a step further would suggest that higher crystallization temperatures produce lower amorphous orientation and, perhaps, fewer tie molecules. Lower crystallization temperatures would allow greater molecular orientation to be retained and perhaps more tie molecules. This would be one explanation for the high tensile strengths developed under optimum filament spinning conditions for some of the lower molecular weight resins.

An experimental correlation was previously found between the observed tensile strength and the measured birefringence for melt-spun filaments prepared from zniPP resins.[5,6] As the total birefringence increased, the tensile strength was observed to increase. A similar strong correlation was found for the present results for filaments spun from miPP resins as shown in Figure 10. It is also noteworthy that the data in Figure 10 fit in a narrow band, regardless of the molecular weight or MWD. The present results further validated the relationship between the overall molecular orientation and the fiber tensile strength.

Because the major contribution of crystals is to simply act as physical crosslinks to tie the molecules together, it is likely that the noncrystalline portion of the birefringence is the key component that produces the correlation between the tensile strength and total birefringence. The results in Figure 11 show the fiber tensile strength plotted against the noncrystalline orientation function for each fiber sample. Figure 11 indicates that a reasonable correlation exists between the orientation of the noncrystalline chains and the strength of the fiber. However, the results in Figure 11 do not form a band quite as narrow as the data in Figure 10, perhaps because of experimental error. The birefringence was directly measured using a compensator. On the other hand, the noncrystalline orientation function was determined using a combination of wide angle X-ray diffraction, density, crystallinity, and birefringence measurements. Therefore, there were several possible experimental errors involved in the measurement of each data point in Figure 11. Nevertheless, the results were consistent enough to indicate that the tensile strength was correlated to the value of the noncrystalline orientation function.

The elongation to break (ETB) data were expected to be roughly the inverse of the tensile strength. The added strength produced by more tie molecules, greater molecular extension, and higher molecular orientation was offset by the

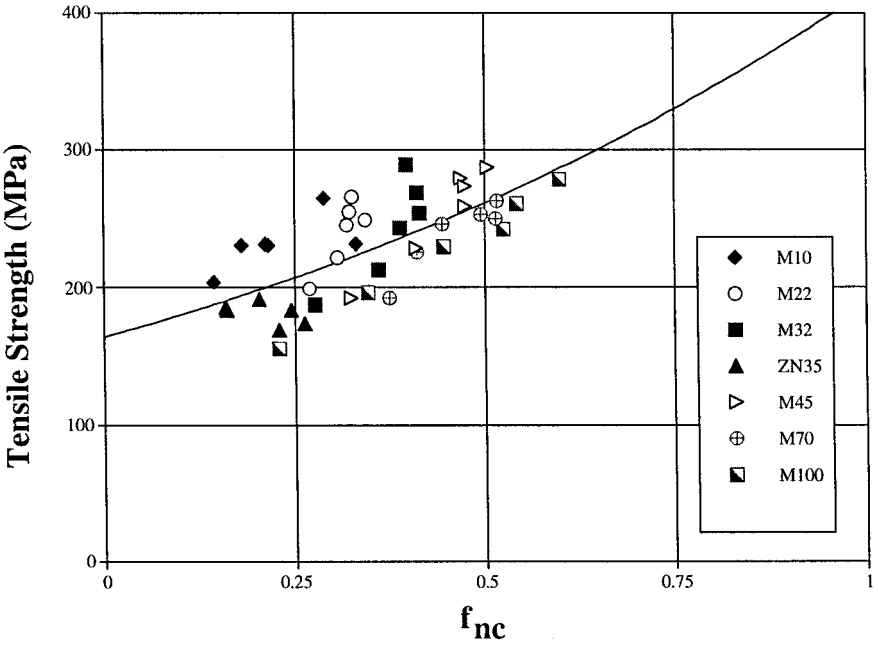

Figure 11 The fiber tensile strength versus the noncrystalline orientation function.

fact that the taut tie molecules did not draw as far before fracture upon uniaxial extension. The data in Figure 12 show the ETB versus the spinning speed. The data indicate that as the spinning speed was increased, the ETB was decreased because of greater orientation and extension as the spinning speed increased. The only seemingly odd behavior in this graph is the position of M10. The M10 resin would be expected to have a slightly higher ETB based on its relative position in the tensile strength data. However, M10 had a very high density, which could have influenced the elongation of the fibers under uniaxial extension.

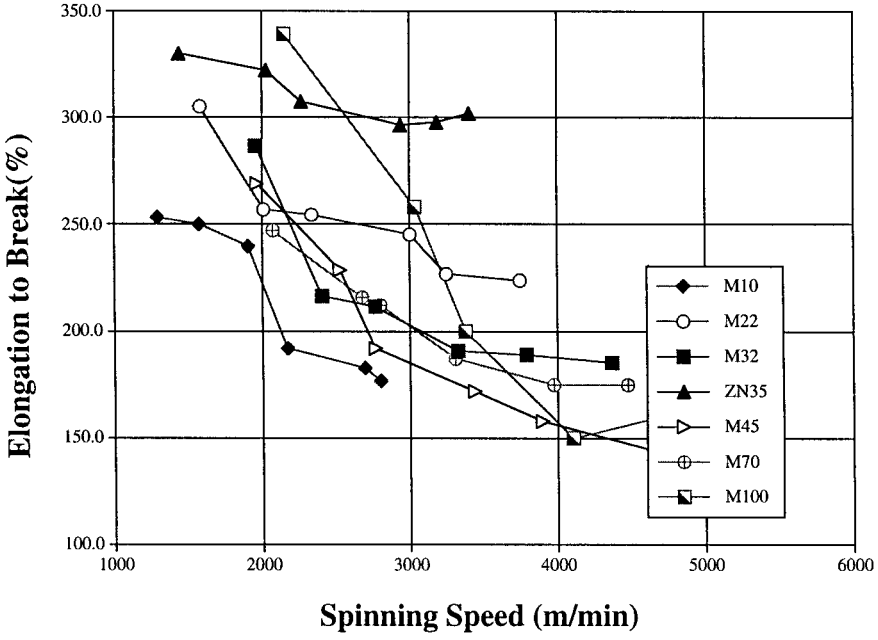

Figure 12 The elongation to break versus the spinning speed.

CONCLUSIONS

The results of this study showed that the average molecular weight and the MWD of miPP resins had significant influence on the structure and properties of melt-spun filaments prepared from the resins.

The density measurements showed that as the spinning speed and molecular weight increased, the as-spun filament density increased. Slight variations in this trend were observed for ZN35 and M45. These variations were explained by the broader MWD of these resins. The fiber density increased as a function of the spinning speed and molecular weight that was due to crystallization occurring at higher temperatures, which allowed more time for the fiber to crystallize and for the crystals to be perfected before the molecular mobility became too low.

The as-spun filament birefringence values showed that the birefringence increased as the spinning speed increased. Further, the maximum filament birefringence increased as the molecular weight decreased. The orientation function results showed that as the molecular weight decreased, the noncrystalline orientation function increased and the crystalline orientation function decreased at a given spinning speed. The orientation functions were both generally increased as the spinning speed increased with the exception of M10 and ZN35. The tensile strength showed a similar trend; as the molecular weight decreased, the maximum tensile strength increased. A very strong correlation was found between the birefringence and the tensile strength. A correlation was also observed between the noncrystalline orientation and the tensile strength. The tensile strength was strongly dependent on the number of tie molecules connecting the various crystallites. It was also somewhat dependent on the crystallinity, in that the number and size of the crystals also influenced the tensile strength because the crystallites acted as an anchoring point for the tie molecules. If the population of crystallites is small or they are very thin, the tie molecules may easily pull out of the crystal, yielding weak filaments.

The tensile modulus is a function of both the crystallinity and molecular orientation. Clearly, the present results showed that the tensile modulus was determined primarily by the spinning speed at which the fibers were spun. It was observed that as the molecular weight decreased, the filaments were less crystalline but exhibited higher overall molecular orientation. Thus, the combined effects of changes in the crystallinity and orientation with changes in the molecular weight tended to offset each other.

The ETB data exhibited behavior that was approximately the inverse of the tensile strength data. This was again attributed to the behavior of the tie molecules. As the number, orientation, and extension of the tie molecules increased, the ETB decreased because less extension and drawing was allowed before rupture or pull out of the molecules and specimen failure.

The authors wish to thank ExxonMobil Chemical Company for supplying the resins, for financial support of this research, and for supplying molecular characterization and viscosity data on the resins. We are particularly indebted to J. C. Randall, Allan Stahl, C. Y. Cheng, and G. C. Richeson for numerous discussions of significant issues related to this research.

REFERENCES

1. Shimizu, J.; Okui, N.; Kikutani, T. In High Speed Fiber Spinning; Ziabicki, A., Kawai, H., Eds; Wiley-Interscience: New York, 1985, p. 429.
2. Fan, Q.; Xu, D.; Zhao, D.; Qian, R. J Polym Eng 1985, 5, 95.
3. Lu, F.-M.; Spruiell, J. E. J Appl Polym Sci 1987, 34, 1521.
4. Lu, F.-M.; Spruiell, J. E. J Appl Polym Sci 1993, 49, 623.
5. Misra, S.; Lu, F.-M.; Spruiell, J. E.; Richeson, G. C. J Appl Polym Sci 1995, 56, 1761.
6. Spruiell, J. E.; Lu, F.-M.; Ding, Z.; Richeson, G. C. J Appl Polym Sci 1996, 62, 1965.
7. Bond, E. B.; Spruiell, J. E. J Appl Polym Sci, to appear.
8. Hermans, P.; Platzek, P. Kolloid-Z 1939, 88, 68.
9. Hermans, P.; Hermans, J.; Vermaas, D.; Weidinger, A. J Polym Sci 1947, 3, 1.
10. Wilchinsky, Z. W. In Advances in X-Ray Analysis; Mueller, W. M.; Fay, M., Eds.; Plenum: New York, 1963; Vol. 6, p 231.
11. Alexander, L. E. X-Ray Diffraction Methods in Polymer Science; R. E. Krieger Publishing Company; New York, 1979; p 241.
12. Stein, R.; Norris, F. J Polym Sci 1956, 21, 381.
13. Stein, R. J Polym Sci 1969, A27, 1021.
14. Samuels, R. J Polym Sci 1965, A3, 1741.
15. Ballou, J.; Silverman, S. Text Res J 1944, 14, 282.
16. Samuels, R. J Polym Sci 1968, 6, 1101.
17. Bruckner, S.; Meille, S. V. In Polypropylene—An A to Z Reference; Karger-Kocsis, J., Ed.; Kluwer Academic: Dordrecht, 1999; p 607.
18. Phillips, R. A.; Wolkowicz, M. D. In Polypropylene Handbook; Moore, E. P., Ed.; Hanser/Gardener Publications: Cincinnati, OH, 1996; p 141.
19. Bond, E. B.; Spruiell, J. E. J Polym Sci Part B: Polym Phys 1999, 34, 2783.